

Carrier capture in InGaN quantum wells and hot carrier effects in GaN

F. Binet ^{a,*}, J.Y. Duboz ^a, C. Grattapain ^a, F. Scholz ^b, J. Off ^b

^a *Laboratoire Central de Recherches, Thomson-CSF, 91404, Orsay Cedex, France*

^b *4. Physikalisches Institut, Universität Stuttgart, D-70550, Stuttgart, Germany*

Abstract

Two new aspects of photoluminescence in GaN and alloys are presented. First, quantitative photoluminescence is carried out in a double InGaN/GaN quantum well structure. By comparing the luminescence intensities from both wells, we could extract the recombination velocities in both wells. We show that the capture is more efficient in a deeper well. Second, photoluminescence under strong excitation density is studied. Hot carrier phenomena are clearly demonstrated. From the high energy tail, we determine the electron temperature and we show that the main energy relaxation mechanism is the optical phonon emission. The effect of carrier temperature on the phonon replica on the low energy side of the luminescence peak is also emphasized. © 1999 Elsevier Science S.A. All rights reserved.

Keywords: Photoluminescence; GaN; Quantum

1. Introduction

The spectacular development of the GaN field is in large part due to the optical emission in the near ultraviolet and blue region [1]. Thus, the recombination in GaN layers and InGaN/GaN quantum wells has been intensively studied [2]. However, the great majority of luminescence experiments in GaN/InGaN quantum wells are based on excitation in the GaN barriers and the transfer from the barrier to the well of the photogenerated carriers is seldom studied [3]. In a previous experiment, we showed that the diffusion length of excitons in GaN at low temperature was about 0.1 μm [4]. Here, we want to address the problem of the exciton capture in InGaN/GaN quantum wells. This is done by comparing the photoluminescence of two different quantum wells in different illumination configurations. This will be developed in the first section. Another point of interest is the luminescence in GaN under strong excitation, with carrier densities in the range of those observed in laser structures. However, we worked in a photoluminescence geometry

rather than in a photopumping geometry in order to avoid stimulated emission and optical resonances. Of particular interests are the carrier temperature and the mechanisms which govern the energy relaxation in GaN. This point is addressed in the second section.

2. Carrier capture in GaN/InGaN quantum wells

The main idea here is to compare the luminescence of two different quantum wells (QW1 and QW2) grown in the same sample (QW2 is grown first) and illuminated from the front side or the back side. The solution of the diffusion equations and its comparison with experimental luminescence allow us to determine the well recombination velocities.

The sample was grown by metal organic vapor phase epitaxy on a sapphire substrate and a low temperature AlN buffer layer [5]. QW2 (QW1) was designed to have 13% (6%) In and both wells were 3 nm thick. Two 0.4 μm -thick GaN layers are grown below QW2 and on top of QW1. This thickness is larger than the pump absorption length (about 0.14 μm for a HeCd laser at a wavelength of 325 nm). Thus, we can consider that carriers are created in the top (bottom) GaN barrier when the sample is front (back) side illuminated. These

* Corresponding author. Tel.: +33-1-69339387; fax: +33-1-69330740.

E-mail address: binet @ thomson-lcr.fr (F. Binet)

layers remain sufficiently thin so that carriers can diffuse towards the wells as the diffusion length is about $0.1 \mu\text{m}$ at low temperature [4]. The GaN barrier between wells is chosen as thin as possible (20 nm) so that volumic recombination is reduced. As we want to study the electron recombination from the luminescence, it is of prime importance to unambiguously identify the origin of the luminescence. For this purpose, we performed first a secondary ion mass spectroscopy (SIMS) analysis of the sample and measured the relative In content as a function of depth. The SIMS spectrum with arbitrary units is shown in Fig. 1. We observe that both wells are clearly separated and that the In content in QW2 is about twice that in QW1. Then, three different craters were etched by the Cesium ion beam and controlled by the SIMS analysis so that the etched surface was right on top of QW1, in the barrier between both wells, and right below QW2, respectively. The luminescence is observed with a selective excitation in each crater, as shown in Fig. 2. We can thus conclude without any ambiguity that QW1 emits at about 3.27 eV while QW2 emits around 3 eV. Furthermore, there is only one peak associated with each quantum well and all the intensities in a given peak arise from only one well.

The second step was to measure the photoluminescence in the sample with front side and back side excitations, the luminescence is collected in both cases from the front side. Spectra at 4 K are presented in Fig. 3. We observe the band edge of GaN and two lines attributed to QW1 and QW2, at 3.27 and 3 eV, respec-

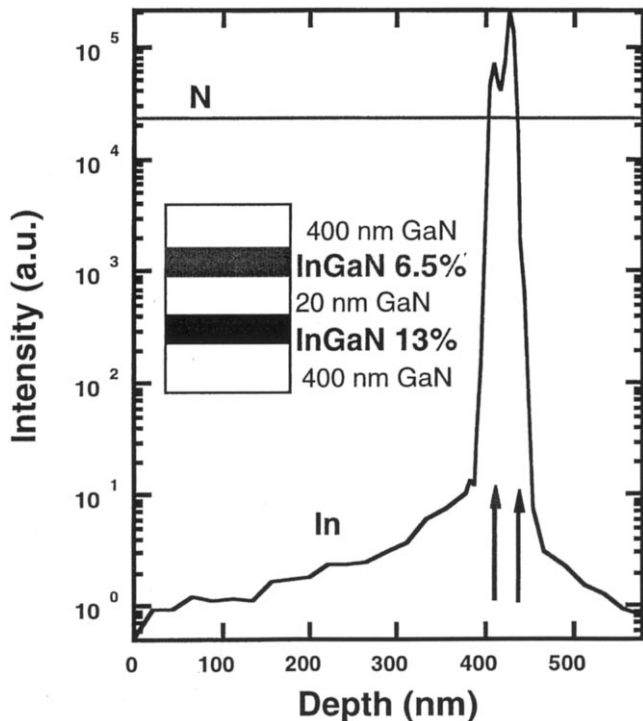


Fig. 1. SIMS profiles of the double InGaN quantum wells sample.

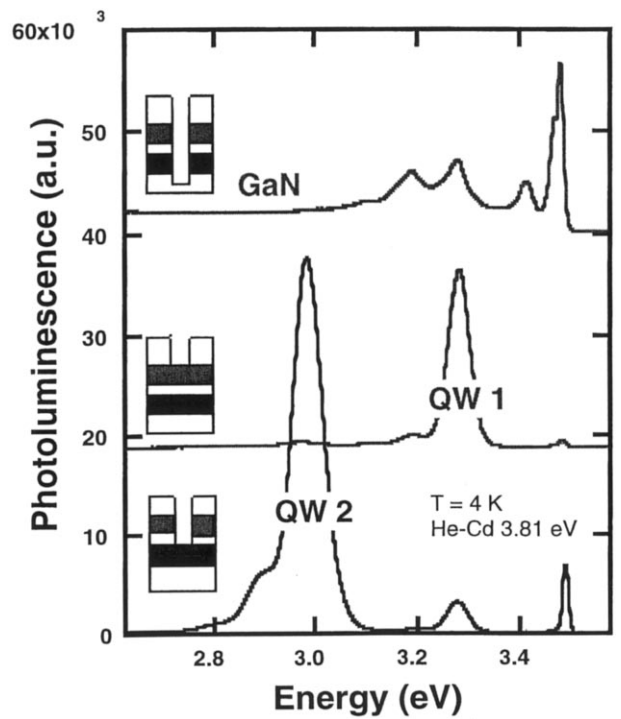


Fig. 2. Selective excitation of different layers of the sample. The excitation beam is located in three different craters etched by the Cesium ion beam of the SIMS.

tively. As expected, the ratio of luminescence between QW1 (I_1) and QW2 (I_2) is larger in front side than in back side excitation geometry. We could integrate the intensity under each peak and we found that the ratio $I_1/I_2 = 0.83$ and 0.30 for front side and back side, respectively, with an uncertainty of about 10%.

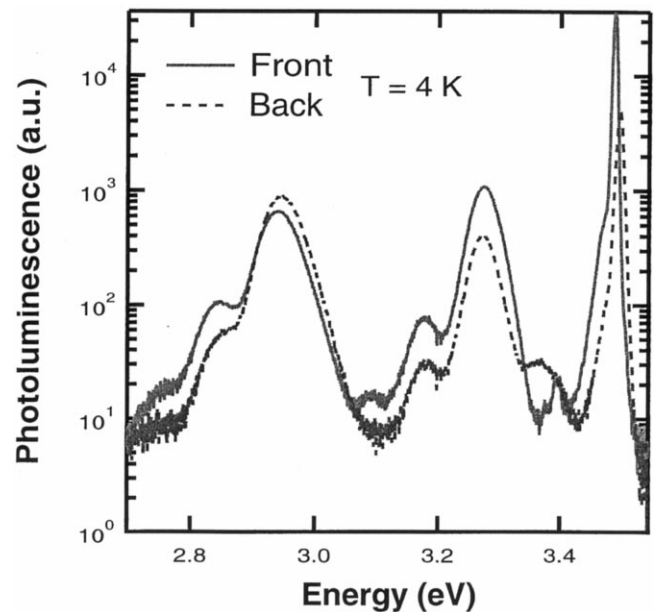


Fig. 3. Photoluminescence spectra of the frontside and backside illuminated sample at 4 K.

The analysis is based on the diffusion equations in the samples. We consider that all the absorptions and thus the carrier photogenerations occur in the top (or bottom) GaN barrier and the wells are described as planes at position h and k from the surface ($h = 400$ and $k = 420$ nm). In stationary regime, the carrier conservation leads to the following equation:

$$\frac{\partial n}{\partial t} = 0 = -\frac{n}{\tau} + D \frac{\partial^2 n}{\partial x^2} + G \quad (1)$$

where τ and D are the exciton lifetime and the diffusion constant, respectively. We define the diffusion length $L_D = (D \times \tau)^{1/2}$. In the intermediate region, the generation term vanishes and the solution can be written as:

$$n(x) = \frac{n(k)}{\sinh\left(\frac{k-h}{L_D}\right)} \sinh\left(\frac{x-h}{L_D}\right) + \frac{n(h)}{\sinh\left(\frac{k-h}{L_D}\right)} \sinh\left(\frac{k-x}{L_D}\right) \quad (2)$$

The recombinations in QW1 [$s_1 n(h)$] and QW2 [$s_2 n(k)$] define the boundary conditions and lead to a relation between the carrier densities at h and k . The luminescence intensities are given by $\eta_1 s_1 n(h)$ and $\eta_2 s_2 n(k)$ in QW1 and QW2, respectively, where η is the radiative efficiency in the well. Finally, the luminescence ratio for front side illumination is given by:

$$\left(\frac{I_1}{I_2}\right)_{\text{front}} = \frac{\eta_1 s_1}{\eta_2 s_2} \left[\left(\frac{L_D s_2}{D} + 1\right) \sinh\left(\frac{k-h}{L_D}\right) + \cosh\left(\frac{k-h}{L_D}\right) \right] \quad (3)$$

An analogous calculation leads to the ratio for back side illumination:

$$\left(\frac{I_1}{I_2}\right)_{\text{back}} = \frac{\eta_1 s_1}{\eta_2 s_2} \left[\left(\frac{L_D s_1}{D} + 1\right) \sinh\left(\frac{k-h}{L_D}\right) + \cosh\left(\frac{k-h}{L_D}\right) \right]^{-1} \quad (4)$$

It is clear from Eq. (3) and Eq. (4) that no information on capture can be extracted from our experiment if $L_D s_i / D \ll 1$ or $s_i \ll D / L_D = L_D / \tau$. In other words, recombination velocities can be deduced only if they are not too small in comparison with the diffusion velocity. The diffusion length has been estimated to be about 0.1 μm [4] and the decay time is usually measured in the range of 100 ps in GaN at 4 K [6,7]. The radiative efficiencies in both InGaN wells are assumed to be equal, the ratio η_1 / η_2 is thus equal to unity. The solutions of Eqs. (3) and (4) lead to recombination velocities $s_1 = 1.6 \times 10^5 \text{ cm s}^{-1}$ and $s_2 = 3.6 \times 10^5 \text{ cm s}^{-1}$. It should be noted that the uncertainty on the lifetime

leads to the same uncertainty on the actual recombination velocities. However, the ratio between s_1 and s_2 is not affected by this uncertainty. The same experiment was performed at higher temperatures. Up to 30 K, the luminescence intensities remain almost the same. This may confirm that the radiative efficiency is equal to unity at low temperature. Above 30 K, the luminescence intensities decrease in a different way in both wells. It is thus likely that radiative efficiencies become less than unity and different in both wells. One additional problem stems from the diffusion length that is not known with accuracy at higher temperature. Hence, the determination of recombination velocities at high temperature was not possible by our method.

At 4 K, we have shown that the recombination velocity increases with the In content or the depth of the well. As the well depth increases, the number of bound levels increases and the scattering (in large part due to LO phonon emission) from barrier states to bound states increases, and so does the recombination velocity. Finally, we found that the recombination velocity is larger than the diffusion velocity which can be estimated to be around 10^5 cm s^{-1} and is smaller than but not negligible compared to the thermal velocity which is about $8 \times 10^5 \text{ cm s}^{-1}$ at 4 K. As a result, the capture in the well is efficient as shown by the large luminescence signals obtained in such InGaN/GaN structures [5,3].

3. High excitation power photoluminescence in GaN

Recombinations in GaN are known to be dominated by excitonic effects up to room temperature [8]. In optically and electrically pumped lasers, however, the carrier density is much larger than that in usual photoluminescence experiments, and the excitonic description may not be relevant anymore [9]. In stimulated emission geometry, spectra are dominated by the exponential amplification of mode with positive gain and by the resonance of optical modes [10]. Thus, we have studied the recombination in GaN under intense excitation in the usual photoluminescence geometry in order to avoid the stimulated emission. We used a quadrupled YAG laser (energy = 4.66 eV) with 10 ns-long pulses and a 20 Hz repetition rate. The pulse duration is larger than characteristic relaxation times so that these measurements are done in the quasi-stationary regime. The recombination coefficient B in GaN has been measured by several groups to be equal to $1.3 \times 10^{-8} \text{ cm}^3 \text{ s}^{-1}$ [11,12]. Given the value of B , the carrier density reached during the pulse ranges from several 10^{17} to a few 10^{19} cm^{-3} . The pump is normally incident on the sample and the luminescence is collected normally and analysed by an Optical Multichannel Analyser. The temperature for this study is kept around 30 K. In Fig.

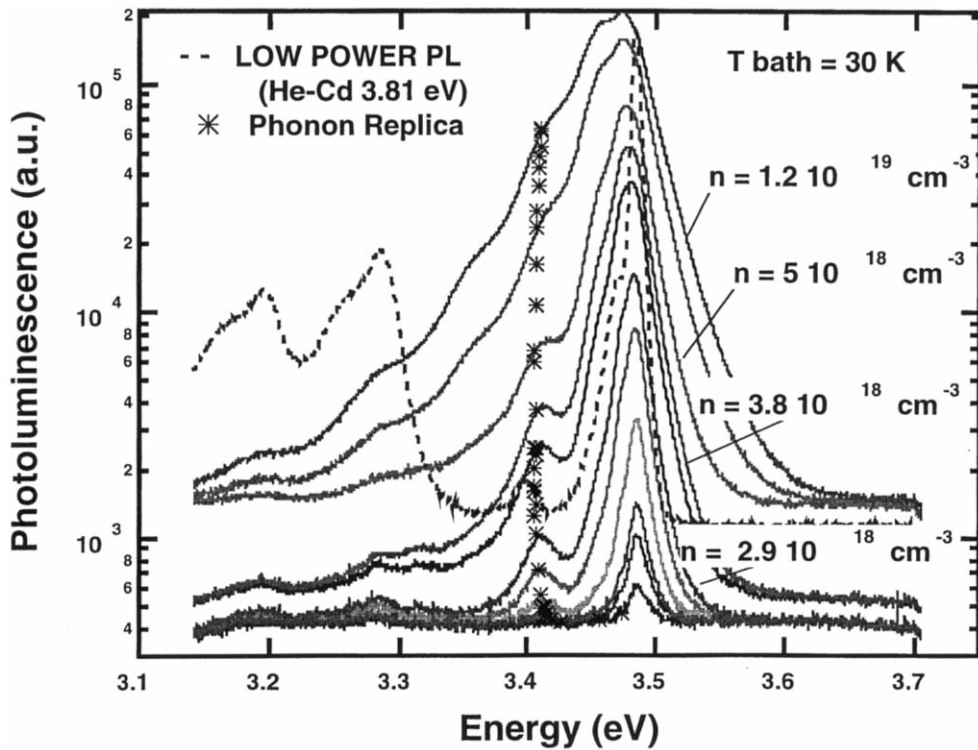


Fig. 4. Photoluminescence spectra of the GaN sample at a bath temperature of 30 K. The dashed spectrum corresponds to the low power photoluminescence spectrum obtained with a CW 3.81 eV He-Cd. The other spectra are obtained with a YAG $\times 4$ laser.

4, we present the spectra obtained for various pumping intensities and also a spectrum obtained in continuous regime at low power with an HeCd laser (3.81 eV). The CW spectrum is dominated by the exciton line at 3.483 eV, the luminescence peaks of the bound and the free excitons cannot be resolved. We note an impurity related line around 3.4 eV and the donor–acceptor line and its phonon replica in the range of 3.2–3.3 eV[13]. Let us now turn to the pulsed excitation experiment. The spectra collected at low power basically present the same features as in CW excitation. However, as the excitation power increases, the spectra are deeply modified. We observe a high energy tail on one side, and many periodic structures on the low energy side.

We first discuss the high energy tail. Fig. 5 is a semi-log plot on the tail, showing the exponential behavior of the luminescence. Let us remind the reader that the emission at energies far above the band gap is expected to follow the relation $I \approx \exp[-(E - \mu)/kT_e]$ where μ is the chemical potential and is equal to the difference between electron and hole pseudo-Fermi levels and T_e is the carrier temperature (we assume here for simplicity that the electron and hole temperatures are equal) [14]. Hence, the slope of the tail in Fig. 5 gives the electron temperature. We observe that it increases with increasing excitation intensity.

In order to interpret the temperature dependence on pump intensity, we have to discuss the different energy

relaxation mechanisms in GaN. The photon absorption at $h\nu = 4.66$ eV creates carriers in the conduction and valence bands with an excess energy equal to $m_r/m_i(E - E_g)$, where m_r and m_i are the reduced and carrier masses, respectively. As the electron mass is smaller than the hole mass, we will concentrate on electrons only. Thus, very energetic electrons are created at 935 meV above the conduction band minimum and can then relax towards less energetic states via two different mechanisms [15]. The first one is the LO phonon emission, the LO phonon energy $E_{LO} = 92$ meV in GaN [16]. After the emission of 10 phonons (i.e. 920 meV), the remaining energy of 15 meV can be dissipated by acoustic phonon emission or by electron–electron interaction. The second mechanism is the collision of the energetic electron with a cooler electron which results in a redistribution of the energy among electrons. One can theoretically calculate that the collision rate with a cooler electron increases with the carrier density while the LO phonon emission rate remains constant [15]:

$$\left(\frac{d\varepsilon}{dt}\right)_{e-e} = \frac{n\varepsilon^4}{4\pi K^2(2m_e\varepsilon)^{1/2}\varepsilon_0^2} \quad (5)$$

$$\left(\frac{d\varepsilon}{dt}\right)_{e-LO} = \frac{2eE_0E_{LO}}{(2m_e\varepsilon)^{1/2}} \left[N_q sh^{-1} \left(\frac{\varepsilon}{E_{LO}} \right)^{1/2} - (N_q + 1) sh^{-1} \left(\frac{\varepsilon - E_{LO}}{E_{LO}} \right)^{1/2} \right] \quad (6)$$

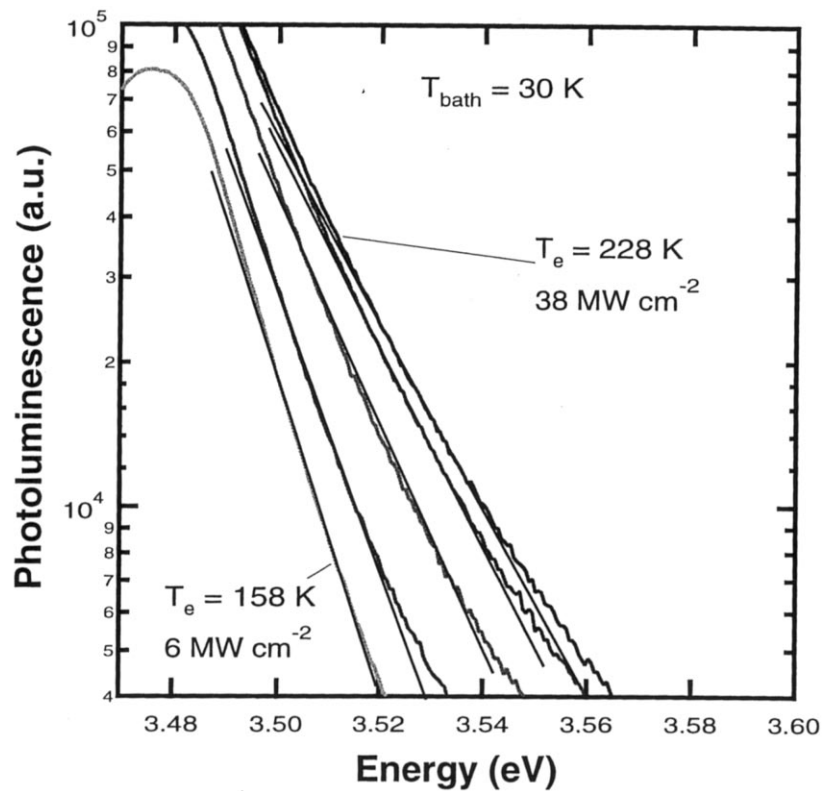


Fig. 5. Semilog plot of the high energy tail of the photoluminescence spectra at different power densities, the carrier temperature is deduced from the slope.

where E_0 is the electrical field associated with the LO phonon, K an average dielectric constant, ϵ_0 the free space permittivity, ϵ the energy of the photoexcited electron and N_q the phonon population term. In GaN, the electron reduced mass = 0.22 [16], K is taken to be 7.4 [17] and the calculation of the electrical field (eE_0) gives 0.33 MeV cm^{-1} . Above a critical density evaluated to be $2.5 \times 10^{19} \text{ cm}^{-3}$, electron–electron collisions prevail while LO phonon emission is dominant below this density [15]. However, as the electron energy decreases, the situation may change. The actual result is that a noticeable fraction W/E_{excess} of the initial excess energy is given to the electron gas. At this point, two cases must be considered. If electron–electron collision rate is larger than LO phonon emission rate, then the electron population relax towards a Maxwellian hot electron gas with an electron temperature T_e which is larger than the lattice temperature. On the contrary, if electrons lose their energy faster than they exchange energy between each other, then an electron temperature cannot be defined. Again, the comparison between LO phonon emission and electron–electron collision rates shows that a certain carrier density must be reached so that we get a hot electron gas with a well defined electron temperature [15]. We can show that this is the case in the range of densities involved here. The situation is thus, a hot electron gas which cools by

LO phonon emission. In the stationary regime, we can write a balance equation for the hot electron gas between the energy lost by phonon emission and the energy gained by the photogeneration of high energetic electrons [15]:

$$\frac{I}{nd} \frac{W}{h\gamma} = \frac{2E_{\text{LO}1/2}}{(m_e)} eE_0 \exp\left(-\frac{E_{\text{LO}}}{kT_e}\right) = \frac{E_{\text{LO}}}{\tau} \exp\left(-\frac{E_{\text{LO}}}{kT_e}\right) \quad (7)$$

where d is the larger of the diffusion or the absorption length, I is the excitation density and n is the carrier density. The time τ that is defined through the previous equation cannot be considered as a simple LO phonon emission time but rather an effective time that takes into account electron–electron collision and phonon emission in a hot electron gas [14]. For GaN, it can be calculated to be 7 fs. Let us remark that this value is much smaller in many other semiconductors (for instance, $\tau = 130 \text{ fs}$ in GaAs), indicative of the more ionic bonds and the larger LO phonon coupling in GaN [18]. Experimentally, we have studied the dependence of the electron temperature deduced from the high energy tail on the excitation power density. The result is shown in Fig. 6. We observe that the inverse of the electron temperature varies exponentially with the excitation power, and the slope is 90.9 meV which is very close to the LO phonon energy [19]. In order to fit

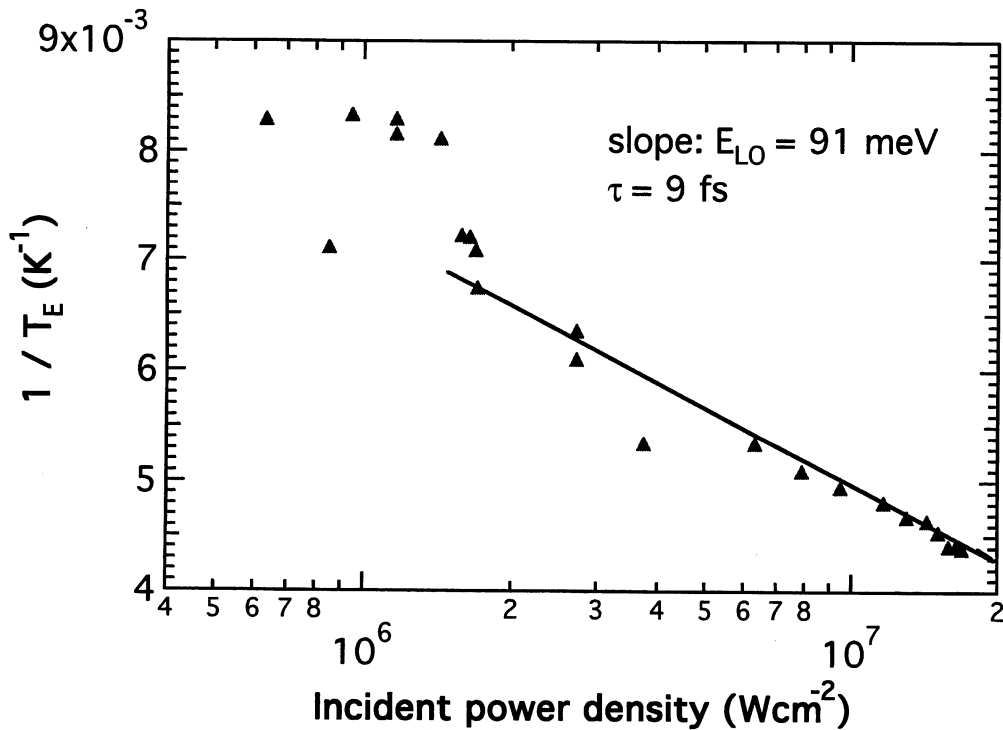


Fig. 6. Arrhenius plot of the incident power density as a function of the carrier temperature at a bath temperature of 30 K. The slope obtained from the fit gives the GaN LO phonon energy.

the data, we have to use an effective time $\tau = 9 \text{ fs}$. Given the theoretical approximations, there is a very good agreement between theory and experiment. Fig. 6 is a direct evidence of the limitation of the hot electron temperature by LO phonon emission. The density ranges here from 10^{18} to 10^{19} cm^{-3} . In this range, the calculation shows that electron–electron collision are dominant in the electron gas so that an electron temperature can be defined. Below $2 \times 10^{18} \text{ cm}^{-3}$ (about 0.8 MW cm^{-2}), the electron temperature does not follow the exponential law anymore, this is due to the Mott transition and to excitonic effects at lower densities [8]. Another possible limitation of the theory presented here is the coupling between electron–electron interaction and phonon emission when the plasmon energy equals the phonon energy [20]. This occurs for a density $> 6 \times 10^{18} \text{ cm}^{-3}$. However, we do not observe experimentally any deviation from the simple theory up to a density of 10^{19} cm^{-3} , and we thus do not see any plasmon effect on the electronic temperature.

4. Conclusion

Two aspects of the recombination in GaN and alloys have been studied. We have quantitatively shown

that the capture of electron-hole pairs in InGaN quantum wells is efficient and the capture velocity increases with the depth of the well. Also, we have studied the recombination in GaN under high excitation. A hot electron gas has been proven to exist and has been characterized. Its temperature is controlled by LO phonon emission.

References

- [1] S. Nakamura, et al., Appl. Phys. Lett. 70 (1997) 868–870.
- [2] S. Chichibu, T. Azuhata, T. Sota, S. Nakamura, Appl. Phys. Lett. 69 (1996) 4188–4190.
- [3] E.S. Jeon, et al., Appl. Phys. Lett. 68 (1996) 4194.
- [4] J.Y. Duboz, et al., Diffusion length of photoexcited carriers in GaN, EMRS/ICAM 1997, Mater. Sci. Eng. B 50 (1997) 289–295
- [5] A. Sohmer, MRS Internet Journal of NSR 2 (1997).
- [6] J.S. Im, et al., Appl. Phys. Lett. 70 (1997) 631–633.
- [7] C.I. Harris, B. Monemar, H. Amano, I. Akasaki, Appl. Phys. Lett. 67 (1995) 840–842.
- [8] S. Chichibu, T. Azuhata, T. Sota, S. Nakamura, J. Appl. Phys. 79 (1996) 2784–2786.
- [9] P. Rees, C. Cooper, P. Blood, P.M. Smowton, J. Hegarty, Electron. Lett. 31 (1995) 1149–1150.
- [10] F. Binet, et al., Appl. Phys. Lett. (1997) (to be published).
- [11] F. Binet, J.Y. Duboz, E. Rosencher, F. Scholz, V. Härle, Appl. Phys. Lett. 69 (1996) 1202–1204.
- [12] J.F. Muth, et al., Appl. Phys. Lett. 71 (1997) 2572–2574.
- [13] R. Dingle, M. Ilegems, Solid State Commun. 9 (1971) 175–180.

- [14] S.A. Lyon, *J. Lum.* 35 (1986) 121–154.
- [15] J. Shah, *Sol. Stat. Elec.* 21 (1978) 43–50.
- [16] D.K. Gaskill, L.B. Rowland, K. Doverspike, in: J.M. Edgar (Ed.), *Properties of Group III Nitrides*, INSPEC Production, London, 1994.
- [17] F. Demangeot, et al., *J. Appl. Phys.* 82 (1997) 1305–1309.
- [18] K.T. Tsen, et al., *Appl. Phys. Lett.* 71 (1997) 1852–1853.
- [19] M. Giehler, M. Ramsteiner, O. Brandt, H. Yang, K.H. Ploog, *Appl. Phys. Lett.* 67 (1995) 733–735.
- [20] S. Das Sarma, J.K. Jain, R. Jalabert, *Phys. Rev. B* 41 (1990) 3561–3571.